IC/93/264

INTERNATIONAL CENTRE FOR THEORETICAL PHYSICS

ABLATION OF POLYMERS BY ULTRAVIOLET PULSED LASER

A. Brezini

F. Hamdache

and

N. Benharrats

INTERNATIONAL ATOMIC ENERGY AGENCY

UNITED NATIONS EDUCATIONAL, SCIENTIFIC AND CULTURAL ORGANIZATION

MIRAMARE-TRIESTE

IC/93/264

International Atomic Energy Agency
and
United Nations Educational Scientific and Cultural Organization
INTERNATIONAL CENTRE FOR THEORETICAL PHYSICS

ABLATION OF POLYMERS BY UILTRAVIOLET PULSED LASER

A. Brezini
Laboratoire de Physique Electronique du Solide, U.S.T.O.,
B.P. 1505, Oran El-Mnaouer, Algeria,

F. Hamdache [1]
International Centre for Theoretical Physics, Trieste, Italy

and

N. Benharrats
Institut de Chimie Industrielle,
Laboratoire de Physique Electronique du Solide, U.S.T.O.,
B.P. 1505, Oran El-Mnaouer, Algeria.

ABSTRACT

The surface modifications of different polymers treated by far UV-Excimer laser (λ = 193nm, 248, 308nm) are analyzed by X-Ray Photoelectrons Spectroscopy. The main feature observed depends strongly on the absorption coefficients. For the high absorbing polymers such (PVC, PS, PI, ...) the mechanism of the UV-Excimer Laser interaction appears to be governed by an ablative photodecomposition process (APD) with an APD threshold. In the other limit, i.e. low absorbing polymer the interaction leads to a photothermal process.

MIRAMARE - TRIESTE
August 1993

[1]Permanent address: Laboratoire de Physique Electronique du Solide, U.S.T.O., B.P. 1505, Oran El-Mnaouer, Algeria.

I- INTRODUCTION.

The capability of UV radiation to modify polymer surfaces by photodegradation, photooxidation has already been demonstrated [1-5]. These studies mainly used light of wavelength greater than 193 nm, that penetrates well below the polymers surface inducing photodegradation of the structure. Far UV radiations (180nm<λ<200nm), which has a small penetration depth in organic solids is more adapted to study modifications of the surface and thin films.

The energy of a far UV-photon (>6ev) exceeds the energy of most covalent bonds in the polymer chain and then present a high probability of bond breaking.

From the fundamental point of view, pulsed UV laser treatment have a high energy, so they provides a photochemical process. The pulsed laser also, introduces two different mechanisms [5]: a photothermal energy conversion dominant at long wavelenghts, i.e. λ = 308nm, or a direct photochemical process at shorter wavelengths such λ = 193nm or λ = 248nm. In a photothermal process the photon energy is transformed into lattice vibrations (phonons), either directly or by de-excitation from any laser induced excited states, wheter electronic or excitonic...

When the photons are delivered in an intense pulse of short duration, the concentration of fragments in the irradiated volume reaches a high value, which when it exceeds a threshold level, results in the spontaneous ejection of the fragments into the gas fragments [9-14]. This process is "ablative photodecomposition" introduced in 1982; the ablated materials carries away a high percentage (≅ 95%) of the energy of the photon which is not consumed in the bond breaking. the etching process has led to many potential applications in technology of particular importance. We shall examine the nature of the interaction of pulsed UV at 193nm, 248 and 308nm as a function of fluence with a

variety of polymers.
We have investigates the surface modification of a class of common polymers: the high absorbing polymers like (PVC, PS, PI, PET) and for comparison, results are also reported for low absorbing polymers (PVF_2, PMMA).

II- Optical Properties of Polymers.

II-1- Mechanism of UV absorption .

Synthetic organic polymers are made up of molecules which consist of typically 10^3 to 10^5 atoms, in most cases Carbon, Hydrogen, Oxygen, Nitrogen, etc... A small molecular unit, or monomer, of 6 to 40 atoms is repeated over and over a chain to built a polymer. In fig.21, some particular polymers called poly(ethylene terephtalate) PET, Polyimide PI, poly(methyl methacrylate) PMMA, polycarbonate PC, Polystyrene PS,... are reported along the monomer units in each case. A polymer is constituted by 10^2 to 10^3 monomer units. The nature of the bonding between atoms within a polymer is covalent, i.e shared electrons, and rather strong, namely 60 to 150 kcal/mol. However, the energy binding of the molecules are weak, typically less than 10kcal/mol. Absorption of photons of ultraviolet (UV) wavelength is efficient in exciting the bonding electrons in polymers. The phase diagram in fig.24 describes the absorption of a UV photon by one bond X-Y in the molecule. The lowest broken curve describes the lowest energy state for the bond and where the horizontal lines represent the vibronic states. The processus of the absorption of a UV photon (vertical arrow 1) is such fast that the nucleus remain unrelaxed in their initial configuration, and leads to an upper electronic level. This resulting state is again a bound state as shown in fig.24 but metastable with respect to the original state. In the final state, the energy in the bond is greater than the bond energy and therefore the two atoms X and Y can dissociate at the

very next vibration. Indeed, this dissociation processes compete with other phenomena such the fluorescence, the internal conversion (arrow 2 in fig.24), the vibrational deactivation, the intersystem crossing to a different electronic state, the collisional quenching. Therefore the photolysis and photochemical processes that follow electronic excitation are rather complex and a convenient understanting has still to be achieved [21]. In particular, the interaction of the photon with the electrons in the X-Y molecule can lead to a promotion of a valence electron from a bonding to an antibonding orbital, which in the most common process in the wavelength region exceeding 200 nm. In decreasing wavelength, the number of valence excitations increases rapidly and it becomes not obvious to assign absorptions to specific transitions in a polyatomic molecule. Furthermore for wavelengths less than 200 nm, the situation becomes puzzlling since Rydberg transitions play a significant role. In particular, Rydberg transitions result when an electron from a bonding orbital or an electron from an anti-bonding or weakly bonding orbital is promoted to a Rydberg orbital [23]. Usually, in polyatomic organic molecules, almost these transitions can occur simultaneously.

III- LASER ABLATION CHARACTERISTICS.

III-1- Materials- Laser Wavelength and Pulse Characteristics.

An understanding of the processus of laser etching of polymers is of interest from both the macroscopic and microscopic dynamic viewpoints. A simple and convenient source of laser radiation in the UV region became available with the invention of the excimer laser in the seventies. Investigations on the interaction UV pulsed laser with solid organic matter such polymers and

pulsed laser with solid organic matter such polymers and biological tissue led to the discovery in the early 1980's at the IBM T.J. Watson research centre of the phenomenon of "Ablative Photodecomposition" (APD) [2-3,22]. Most of the etching studies were conducted using excimer lasers as the source of UV laser radiation. The appropriate filling of gas with Helium (193 nm) as buffer gas provides the wavelengths of interest from 157 nm to 351 nm. Furthermore the excimer laser pulse width (full width at half-maximum) ranges from 7 to 35 ns. One of the main advantage of these lasers originates from the uniformity of the density energy of the delivered pulses. A wide variety of polymers can be ablated by UV laser pulses. In the following section the UV ablation of PI, PMMA, PET, and PC is reported and the experimental observation from various groups are summerized. The wavelengths used range from 193 nm to 351 nm.

III-2- Intensity Effect And Ablation Condition.

The chemical nature of the reactions that are involved in UV laser ablation of polymers is far from clear. Fragmentation products such as atoms, diatomics, small molecules, and small fragments of the polymer chain are all observed. The ablation process is believed to be a volume explosion which would make the production of small molecules important. The photochemistry of polymers is a well-studied subject, but such studies emphasize reactions at low intensities and ,often, oxidative conditions. For the purpose of the present work it is necessary to take a different approah. We have to distinguish between two very general processes originating from the excited electronic state, created by the absorption of UV laser light.

1/ Photofragmentation leading to stable photoproducts.

2/ The relaxation back to the initial ground state, which merely degrade the energy without engendering any photodecomposition.

The basic idea is the notion of an absorbed photon flux threshold below which fragmentation is negligible. Above this threshold level, photofragmentation may then successfully compete. More precisely the flux ϕ_T, defines the concentration of photons absorbed per unit time.

III-3- Etch deepth, Threshold fluence.

The etching process started when the incident fluence exceed the threshold value. This process depends of the absorption coefficient of the material, and of the wavelength of the UV laser. The etching rate increased with fluence up to about few ten of J/cm^2 and then satured for the studied polymers.
The photodegradation of a polymer by UV laser pulses lead to etching the surface when the power density is sufficient to break up the physical structure of the polymer. The ablation occurs when the fluence exceeds a critical value "ϕ_{th}". This threshold value is quite small for most polymers in the range of few mJ/cm_2 (10 mJ/cm_2 for PMMA at 193 nm) to few hundred mJ/cm_2 (130 mJ/cm_2 for PI at 351 nm). At such fluences the distinction between photochemical and photothermal process and their contribution to the removal rate is not fully understood [25-29]. The threshold values for PI, PMMA, and PET at different wavelengths are listed in table.3.

III-4- Bee'rs Law- Etch Rate dependence.

The penetration of the radiation trough the solid follows a simple relation: the Beer's law:

$$I_t = I_0 \exp(-\alpha l) \qquad (1)$$

The Beer's Lambert relation describes the exponential attenuation of laser intensity under the assumption that a threshold fluence is required to supply the minimum energy or to reach a critical density of broken bonds for ablation at depth X. In the equation (1), I_t and I_0 are the intensities of the beam of light before and after transmission trough a slice of material of tickness l, and α, the absorption coefficient, which is a characteristic property of the material. For most materials, significant etching occurs when the laser fluence is above a threshold, under this condition each pulse ablates the same amount of materials [29-30,]. The etch depth per pulse at any wavelength λ, roughly obeys to the empirical equation.

$$X = \alpha^{-1} * Ln(\Phi_{inc}/\Phi_{th}) \quad (2)$$

Φ_{inc} and Φ_{th} are respectively the incident and threshold fluence. X the depth on the material. The equation (2) derived from the Beer's law. Figs 22-23, shows the etch rate versus the fluence for PI respectively at different wavelength (193,248,308 nm) [31] and (248,308,351 nm) [32]. It appears from this figures the cross over of the curves at fluences above the threshold. The etch depth/pulse versus fluence (fig.22) indicate that the variation is not a linear at λ = 248 nm and 308 nm, whereas the fig.23 exhibit the linear dependance of the same range of the fluence. At fluences higher than the cross-over the etch depth significantly deviates from equation (2) and tend to saturate[33-34]. This is due to the reaction products which interfer with the laser beam and absorb a part of the energy.

III-5- Influence of the pulse duration.

A more standard approach, to the caracterisation of the polymer etching process, consist in the measure of the etch depth versus the number of the pulses, or the pulses duration.

The variation of the etch depth with the number of the pulses is usually linear relation at fluences higher then the threshold fluence. In practice, the depths etched by varying numbers of pulses are averaged. For PC and PMMA [38], fig.21 displays the etch rate versus the number of the pulses at λ = 193 nm in vacumm; the curve is initially irregular and becomes smooth after many pulses. Other groups try to find a relation between the etch depth and the pulses duration. In the literature, it is shown that for PI at λ = 308 nm, there is no significant dependence with pulse width varying from 10 to 80 ns [7] .

IV- Experiments.

IV-1- Materials.

All the experiments reported here were carried out in air atmospher at ambiant room temperature. Samples were all commercially available polymer which were used as received. PVF2 and PVC (from Solvay), were self supporting or solvent cast films from Toluene, Tetrahydrofurane and Dimethylformamide respectively and PS was 2mm thick film (from Johnson and Matthey).Polyimide was free standing film, Kapton films (from Dupont corporation under the trade name of Kapton). Possibly that different preparations of thin films [12] influence the response to UV light. this remark may be kept in mind in comparing with other results.

IV-2- Light source.

The source of UV laser radiation was a Lambda-Physik Model EMG 200 excimer laser. The appropriate filling of argon and Fluorine with Helium as buffer gas was used to provide the wavelength of interest λ = 193nm. The repetition rate of the pulses was kept at

interest λ = 193nm. The repetition rate of the pulses was kept at 3HZ to avoid any cumulative heating effects from a succession of pulses. The pulse duration had full width at halfmaximum of 20ns. The determination of a single pulse energy was obtained by measuring the average power of the laser at 10 HZ operation rate before and after treatments. Energy measurements were made using high-sensibility a gen Tec Joulemeter. The irradiation area was accounted for and a conversion to a single pulse fluence (mJ/cm^2) was performed. Only the central uniform part of the laser output was defined by a slit and concentrated by the use of a spherical quartz-lens. The beam was defined by a 2mm Ø aperture which was in contact with the polymer surface.

IV-3-Mesure Of The APD Threshold .

The threshold fluence for the APD of the polymers has been determined by the quartz crystal microbalance (QCM) method [8]. We have considered the resonance frequencies of an oscillating quartz covered by the polymer film. The difference $\Delta F = F - F_0$ is proportional to the mass lost Δm by the polymer film after one laser pulse via the relation:

$$\Delta F = (2.13 * 10^6 * F^2 * \Delta m) / A$$

Here A describes the irradiated area. The ratio $\Delta m/A$ and F are measured in g/cm^2 and MHZ units respectively. Then the APD threshold may be deduced from the curve ΔF for PVC (Fig. 2a) and PS (Fig.2b), or equivalently mass loss Δm, versus the laser fluence. The main advantage of this method is the very high sensitivity and precision in determining the APD threshold [17]. Towards this end polymers were disssolved and spin-coated on quartz disks to form a film.

IV-4-XPS Analysis.

The XPS analysis measurements were obtained on a Hewlett-Packard 5950 A Photoelectron Spectrometer. The X-ray source was the Alkα (1486.6 ev) emitted by an aluminium anode. At the intensity used no damage to the Polymer surface was observed during analysis. The vacuum in the analysis chamber was kept under 10^{-9} Torr. In the HP 5950 A, the X-ray beam is monochromatized and focused into the sample. This aspect is fundamental for the analysis of insulating materials such as polymers since charging due to loss of electrons is essentially non uniform across the sample and produces a critical loss of resolution [13]. The situation was improved by the use of an electron flood gum and both electron intensity and energy were adjusted until the best resolution was reached for a sample of polymer as received. The spectrometer has been energy calibrated by positioning the main component of the carbon peak (as determined by curve fitting) at 284.9 ev which is considered as the reference.

V-1- Absorption coefficient.

UV absorption coefficient were measured with a Cary 219 Varian Specrophotometer. Observing the UV absorption spectra of the polymer, we differenciate from two regimes :

- The high absorption coefficient for PVC, PI, PS, PET and the low absorption coefficient for PVF_2, PMMA. From figs. 1a and 1b, the 193 nm absorption coefficient deduced appear to be in close agreement with other data [14]. Note that for PS and PI we have considered the value from the literature for α-methyl PS, since the spectrometer range was limited [15-16]. We have also determined from these data the penetration depth of 99% of the laser energy deposited (see table.1). Therefore, it is expected from these observations that the surface modification induced by

laser treatment to be quite different.
The clean etching is observed only for materials with a strong absorption coefficient. Figs.17,18 shows the absorption coefficient versus the wavelengths for PMMA and PI , we observe that the etching of PMMA with excimer laser at λ = 308 nm or λ = 351 nm looks to be a challenge. By sensitizing PMMA with high absorbing doppants [45], the etching is then possible from 193 to 351nm. (Fig.19) PI and PET are strong absorbing materials at the standard excimer laser wavelength (see table.2). The intense absorption of Imide groups in PI suggested interesting possibilities for the process of degradation .

V-2- Refraction Index.

One of the important optical property is given by the index of refraction. Table.4 give the value of refraction for some of study polymers.

V-3- APD Threshold Value .

For the high absorbing polymers PS and PVC, laser treatments were carried out at different fluences from 5.5 to 100 mJ/cm^2. The results for Δf as a function of the fluence are reported in figs.2a and 2b. In particular, one can deduce the threshold fluence about 10 and 28 mJ/cm^2 for PS and PVC respectively.
Above 150 mJ/cm^2 which corresponds to the upper limit for the present QCM experimental set up, we are unable to measure any appreciable mass loss on the detector for PE, PP and PVF_2. Therefore if these polymers exhibit a threshold fluence, it must occur at high fluences.
To check the existence of the APD threshold, we have to look to another procedure. Since the main effect on the APD process consists in ejecting material from the polymer, we have attempted

to pierce from standing films by laser treatments. The mesurable quantity; i.e. the 'etch rate' e.n

$$e.n = d/n$$

Where d designe the tickness of the film (in the present study d is about several tens of µm) and n the number of shots before peircing the film.
The result for PI, PET, PMMA, and PVC are listed in table.3. A significative difference appears betwen small and high absorbing polymers

VI- Nature Of The Ejected Products.

VI-1- Analysis Of Gaseous Etch Products.

Many papers have been published, describing a variety of techniques used to obtain in sight into the ablation and trying to explain the complexity of the processes involved in the laser ablation of polymers. Many collisions and interactions occurs in the ablation plume as it leaves the polymer surface, masking the primary process which lead to the ablation. Reaction products of the ablation of PI, PET, PMMA, and PC have been analyzed by severall technics (Time Of Fligth Spectoscopy and Coupled Gas Mass Spectroscopy). In the following, we present the eject products for each of them:

VI-1-1- Etch Products of PET.

PET etch products have been analyzed by Srinivasan and Leigh [24], using a GC mass spectroscopy. They observ, CO, CO_2, H_2O, C_6H_6 and many other carbon containing species. Dyer and all [32],

found that the major products of PET at λ = 193 nm and 308 nm are CO, CO_2, CH_4, C_6H_6. comparing with the two wavelength, it appear's that the fraction of gaseous products is more important at 308 nm for fluence range ϕ_{th} - $2\phi_{th}$.

VI-1-2- Etch Products Of PI.

PI gaseous etch products have been analyzed by Branon and all [25] with mass spectroscopy GC, CO is the primary gas product followed by CN and HCN. Both benzene and CO_2 are essentially the recombination of reaction product in the gas phase. Conventionnel IR spectroscopy [34] has been used to analyze the products reaction of PI, therefore no gaseous hydrocarbons were oberved. This may due to the fact that any generated hydrocarbons are present in too small concentrations, which can't be detected.
By other techniques [33], it found that H_2, HCN and NH_3 are the product ablation of PI.

VI-1-3- Etch Products Of PMMA.

For this polymer (PMMA), at λ = 193 nm, the ablation products are MMA monomer and CO. For a fluence about 15 mJ/cm_2 at λ = 193 nm the MMA monomer represents a yield of 18% of the etch products but only 1% at λ = 248 nm.
The Time Of Flight Mass Spectrocopy technic showed a prominent ions at λ = 188, 166, 154 and 140 nm as ejected species for the PI, PC, PET. This polymers show the ablation products considerably degraded below the monomer and the products tend to be rougly the same for each one. Table.6 give the possible ions products of the ablation at λ = 248 nm for PI, PET, and PC..

V-1-4- Etch Products Of PC.

The largest peak observed in the PC mass spectrum was due to CO, followed closely by C_2H_2. The other ejected product is the Phen-CH_2 (mass 91), Phen (mass 77), and common-hydrocarbon fragments resulting from the photolysis of gas-phase Phenyl.

VI-2- Physical Characteristics.

VI-2-1- Velocity Of The Etch Products.

Many precise measurement of the etch product velocity and the velocity distributions have been studied. The propagation speed of diatomic products from PI etched at λ = 193 nm was measured to be $4*10^5$ cm/s by studying the temporally and specially resolved emission [35-36]. Devis and all [37] obtained the CH velocity of $4*10^5$ cm/s and C_2 velocity of $2*10^5$ cm/s. This values are close to that given by Srinivasan and all [38]. More precise values were measured by Srinivasan and Deyfuss by Laser Induced Fluorescence (L.I.F) for Time Of Flight (T.O.F) measurement. The velocity of C_2 radical from PMMA etching at λ = 248 nm and 160 mJ/cm_2 ranges from $3*10^5$ cm/s to $1.5*10^6$ cm/s with a velocity distribution sharper than the boltzman distribution. Danielzik and al [39] have measured the velocity distribution of PMMA etch product at λ = 193 nm using the T.O.F mass spectroscopy. They reported that the MMA and light product CO possess the same thermal velocity distribution. Other authors [40], detected for PI two waves of velocities, one faster, around 10^6 cm/s and which appears to be composed by carbon clusters. The other one, is about $2.5*10^4$ cm/s ; it was assigned to the aromatics species.
Small positive ions are formed in the laser focus and are accelerated away from the surface via coulomb repulsion. If gas density in the ablation plume is sufficiently high, large carbon clusters may form. In the less intense part of laser beam , the

products are predominatly neutral atoms [41]. Negative ions are formed by electron to the neutral products.

V-2-2- Profil Velocities Of The Etch Products.

The velocities of positive, negative ions and neutral products from λ = 308 nm laser ablation of PI have been measured by Ulmer and all [44]. The positively charged products are ejected with $\cos^4\theta$ distribution about the normal surface. Neutral and negatively charged products show a $\cos\theta$ angular distribution. All products are ejected with a supersonic velocities with:

Velocity(ion+) > Velocity(ion-)> Velocity(neutral)

VII-XPS RESULTS.

VII-1-XPS Result For PVF_2.

The C_{1s} spectrum of the untreated sample (fig. 3a) was curve resolved into 3 components ; at 290.9 ev (CF_2), 286.4ev ($C-CF_2$) and 285.0 ev (neutral carbon : contamination).
Fig. 3b shows the same C_{1s} spectrum after laser treatment at several fluences. A curve analysis with the 3 same components resulted in the oxidation is further confirmed by the variations of the [O]/[C] and [F]/[C] atomic ratio calculated from O_{1s}, F_{1s} and C_{1s} total are, as a function of the laser fluence (Figs 4a and 4b).
A simple picture of what happens can easily be drawn from these data: around the threshold fluence (e.g. 20 mJ/cm_2) almost no ablation occurs and most of the laser energy is converted into direct bond breaking without ejection of matter. Subsquently, this energy is transformed into heat and the surface temperature

raises. The degradated surface then reacts with air, which causes both the oxidation and loss of aromatic character, i.e. a decrease of the Fluor. At higher fluences,UV light creates enough photochemical bond breaking as to induce a dominating photoablative process. A new fresh surface is then observed on the polymer.

VII-2- XPS Result For PVC.

C_{1s} spectrum of a pure PVC sample normally contains two components of similar intensity whose binding energies are 286.4 ev (C-Cl) and 284.9ev [9].
Fig.5 describes the actual C_{1s} spectrum of PVC as received, An excess of the 284.9ev peak is observed due to a neutral carbon surface contamination and the presence of a high binding energy peak at 288.6ev produced by a solvent, presumably a O-C-O type functionality.
From the knowledge of the bad definition of the polymer and the degradation it undergoes under X-ray exposure during XPS analysis, the details of the C_{1s} spectrum appear obviously to be complicated for investigations. Indeed, we have concentrated our analysis with the overall atomic ratio of Cl,O and C versus laser fluence (fig.6) which may be obtained with a reasonable precision after a short time of analysis.
In increasing the fluence to the fluence threshold (fig.2a) (about 30 mJ/cm^2), the chloride concentration is strongly reduced while above 30 mJ/cm^2 an increase is observed to reach at 400 mJ/cm^2, a plateau 30 % which is still far from the stoechiometrie value for PVC (50%). The mechanism may be depicted as follows : below 50mJ/cm^2 most of the laser energy is observed and remains in the polymer leading to its de-chlorination, well-know under UV and X-ray exposure [11]. Above 50 mJ/cm^2, the APD process starts roughly to be dominant and only above 400 mJ/cm^2 a real fresh surface is obtained after laser treatment.

Oxygen content starts from 9% decreases at 30 mJ/cm^2 and then stabilises near 12%. The presence of oxygen is either due to surface oxidation or produced by the presence of a solvent. The last hypothesis appears more reasonable since an APD regime and a fresh surface after treatment at high fluence is expected.
From UV absorption coefficient ($8*10^3$ cm^{-1} at λ = 193nm), etch rate and visual observation, PVC shows a transient range of fluence above fluence threshold where chemical modifications are induced at the polymer surface. Furthermore at very high fluence regime, PVC is left with a fresh ablated surface.

VII-3- XPS Result FOr PS.

Laser treatments were carried out at different fluences from 5.5 to 100mJ/cm^2. The results for ΔF as a function of the fluence are reported in fig.2b, In particular one can deduce the threshold fluence at about 20 mJ/cm^2.
From XPS analysis the C_{1s} spectra of PS before treatment shows a main peak at 285.0 ev and π-π^* shake-up component [9], accounting for inelastic loss of the ejected photoelectron with the π electronic orbitals of the benzene ring. The C_{1s} laser treatment were resolved into three individual peaks : neutral carbon at 285.0 ev, oxygenated carbon (C-O) around 288.0 ev and shake-up component above 290.0 ev (see fig.7 and 8). In fig.9 we have reported the variation of the ratio [O]/[C] versus laser fluence and the aromaticity, relative number of C-O links in C_{1s} and surface atomic ratio of O and C in PS after laser treatment.
For fluence above 50 mJ/cm^2, the polymer surface displays a normal aromatic character and appears to be insensitive to the laser treatment. The main feature observed is a significant reduction of the aromatic character at $\simeq$ 20 mJ/cm^2. Both the shake-up component dissapear and a peak corresponding to the oxidized carbon at 288.0 ev. This oxidation is supported by overall [O]/[C] ratio behaviour as a function of the laser

fluence.
These observations may be interpreted as follow : below the threshold fluence, most of the laser energy is converted into heat which in turns implies an increase of the surface temperature. Therefore such a surface becomes sensitive and reacts with air leading to the oxidation. Above the threshold, UV light is efficient in producing enough photochemical bond breaking and thus a new fresh surface is observed on the polymer.

VII-4- XPS Result For PI.

The different spectra of C_{1s}, O_{1s}, and N_{1s} were resolved into individual peaks. For our purpose the following convention is adopted. The C_{1s} (C=O) indicates the carbon $_{1s}$ ionization energy of the carbonyl carbon atoms. The symbole Ar (Arene) and Ph (Phenyl) are taken to represent the central and terminal benzene rings, respectively. Therefore C_{1s} (Ar-C=O) and C_{1s} (Ar-H) describe C_{1s} energies of the central Benzene carbon attached to the carbonyl groups and to the hydrogen atoms respectively,while C_{1s} (Ph-N) and C_{1s} (Ph-N) represent C_{1s} energies of a phenyl carbon atoms bonded to nitrogen an hydrogen atoms. Experimental and calculated C_{1s} core levels are compared in Table 5. relative to the lowest binding energy C_{1s} (Ph-H) levels. The calculated energy distribution curve (solid line) and experimental ESCA spectrum (dashed line) have been reported in [18]. The dashed curve at highest binding energy (peak 1) contains the C_{1s} (C=O) levels. The middle curve (peak 2) includes the C_{1s} (Ar-C=O) and C_{1s} (Ph-N) levels. The lowest binding energy curve (peak 3) is composed of a number of C_{1s} (Ph-H) levels which are sufficiently close in energy to be grouped together as a single peak (see fig.10).
Laser treatments were carried out at different fluences from 1.5 to 72 mJ/cm^2 in order to appreciate the surface modifications around the threshold fluence $F_c \simeq$ 18 mJ/cm^2. In addition to the

three peaks described above, the C_{1s} laser treated spectra of the polyimide show a π-π^* shake-up component [19] accounting for inelastic losses of the ejected photoelectrons with the π electronic orbitals of the benzene ring (around 290.6 ev) (see figs. 10,11).

At fluences below the threshold fluence almost no ablation occurs and most of the laser energy is converted into bond breaking without ejection of matter. Thus, this energy is converted into heat leading to a raise of the surface temperature. The degradated surface then reacts with air which produces in fact only minor modifications translating the high thermal stability of the polyimide.

At higher fluences, UV laser radiation becomes effective in creating enough photochemical bond breaking as to induce a photoablative procees. In particular, from figs.12 and 13 the variation of [O]/[C] and [N]/[C] atomic ratios against laser fluence indicates a sensitive decrease of oxygen and nitrogen from the treated surface. These data suggest that oxides of carbon (Co and Co_2) and nitrogen compounds (CN and HCN) are readily lost on laser irradiation producing a carbon-rich surface by treatment. The molecular formula of the polyimide is $C_{22}H_{10}N_2O_5$, by laser irradiation loss of nitrogen compounds and oxides of carbon would lead to a residue of the composition $C_{16}H_6$ [9].

VII-5-XPS Result For PET.

The XPS spectrum of the untreated PET, is displayed in fig.14.a. Carbon and Oxygen peaks can be decomposed by curve fitting in fig.15.a into a core levels whose assignements is as follows:
the C_{1s} (285 ev) aromatic carbon, (286.8 ev) carbon bearin a single oxygen , 289.0 ev carboxylic carbon.
the O_{1s} (532.0 ev) π-bonded oxygen, (533.6 ev) σ-bonded oxygen.
The fig.14.b and fig.14.c, displays XPS spectra of PET surfaces

irradiated at λ=193 nm, for two different fluences. The radiation induces a decrease in the oxygen peak intensity, but the two surfaces obtained with the two different fluences shows similar XPS spectra. The ratio [O]/[C] versus fluence (fig.16) show that for fluences greater than the ablation threshold ($\cong$ 40 mJ/cm^2 per pulse) the ratio [O]/[C] is a constant, although under the thershold fluence, the loss of oxygen increase; so the [O]/[C] decrease. In fig.16, we represent also the variation of the etch depth with the fluence. Both curves give a thershold fluence around $\cong$ 40 mJ/cm^2 per pulse. It is quite obvious that the chemical change is proportionnal to the power of the irradiation source (figs.14b,14c, fig.16). The XPS spectra show that the oxygen loss is linearly dependant on the absorbed energy, so we conclude that when the excimer laser pulse has an energy above the threshold of ablation, which is around 40 mJ/cm^2, the PET surface is ablated (fig.16) and the remaining surface is characterized by a constant chemical composition, which is poorer in oxygen than the initial material. This is caused by the loss of volatile molecule, such Co and Co_2.

After laser ablation (fluence $\cong$ 150 mJ/cm^2) the XPS anlaysis of PET sample, show a net decrease in the [O]/[C]. The [O]/[C] ratios as measured by XPS for PET, PI, PMMA are compared (see table.7.). Laser ablation of PI, under the same conditions causes a greater decrease in the [O]/[C] ratio than for PET and PMMA [50].

VIII-Technological Applications Of Polymers.

The laser radiation in the ultraviolet (UV) region became avaible with the invention of the laser excimer in the 1970's. The interaction of UV laser pulses with organic material such polymers lead to the 'Photoablative Photodecompostion'(APD) in 1982's. So, much attention has been given to the laser

photoablation of polymer films because of the applications to etching process in the microelectronics industry. The pulsed laser ablation for the deposition of thin films of ino ganic materials is rapidly becoming a widely used technology This method was used to product dielectric, ferroelectric, piezzoelectric and superconductors films and semiconductors layers. The polymer are selected for specific applications, as we see, based on their thermal, electrical, mechanical and chemical properties. So, the low-dielectric constant polymers have promising applications in high-density electronic packaging products. So, polyimide (PIS) are widely used in such packages due to their excellent thermal stability, relatively low dielectric constant and good mechanical properties. Thin polymer fims have also been used as resist materials for lithography in microelectronics technologies since the 1960's, and the most attractive advantage of an ultrathin resist is to allow electron penetration when the Scanning Tunneling Microscopic (STM) is used. So, due to the absence of any significant damage in unexposed regions, ablation of organic polymers and biological substances with pulsed excimer laser radiation provide a large interest and applications in microelectronic,lithography and surgical applications [48-51] .

Acknowledgments

One of the authors (F.H.) would like to thank Professor Abdus Salam, the International Atomic Energy Agency and UNESCO for hospitality at the International Centre for Theoretical Physics, Trieste.

REFERENCES.

1- R.Srinivasan, "Laser-Processing and diagnostics" in Springer-Series in Chemical Physics, Vol. 39, Ed. D.Brauer, (Springer-Verlag, New-York); 343(1984).

2- R.Srinivasan and V.Mayne-Benton, Appl.Phys.Lett. 44, 576(1982).

3- R.Srinivasan and W.J.Leigh, J.Amer.Chem.Soc. 104, 6784(1982).

4- T.F.Deutsh and M.W.Geis, J.Appl.Phys. 54, 7201(1983).

5- E.Occhiello, F.GArbassi and V.Malastester, Appl.Macrom.Chem.Phys. 169, 143(1989).

6- G.Koren and J.Yeh, J.Appl.Phys. 56, 2120(1984).

7- J.T.C. Yeh, J.Vac.Sci.Technol. A4, 653(1986).

8- S.Lazare, J.C.Soulignac, P.Fragnaud, Appl.Phys.Lett. 50, 624(1987).

9- J.Riga, J.J.Pireaux and J.Verbist, Molecular Physics 34,131(1977).

10- A.Brezini, Phys-Stat.Sol(a), 127, K9(1991).

11- S.Lazare and R.Srinivasan, J.Phys.Chem. 90,2124 (1986).

12- J.H.Branon, J.R.Lankard, A.I.Baise, I.Burns and J.Kaufman, J.Appl.Phys, 53, 2038(1985).

13- D.Briggs, Practical Surface Analysis By Auger and X-Ray Photoelectrons Spectroscopy (Willey, N.York), 359(1983).

14- H.R.Philipp, H.S.Scole, Y.Lin, T.Sitnik, Appl.Phys.Lett, 48(2), 192(1986).

15- H.S.Cole, Y.S.Lin,H.R.Philipp, Appl.Phys.Lett, 48(1), 76(1988).

16- M.C.Bunell, Y.S.Lin, H.S.Cole, J.Vac.Sci and Technol. A4,(6), 2459 (1986).

17- A.Brezini, F.Hamdache, Phys.Stat.Sol.(a) 133, K41 (1992).

18- A.R.Rossi, P.N.Janda, B.D.Silverman aand P.S.Ho, Organometallics 6,580(1987).

19- J.Riga, J.J.Pireaux and J.Verbist, Mol.Phys.34,131 (1977).

20- R.Srinivasan, B.Braren, and R.W.Dreyfus, J.Appl>Phys. 61,372 (1987).
21- J.G.Galvert, J.N.Pitts, Photochemistry, Ed. Wiley. New-York, 1966.
22- R.Srinivasan, Polymer 23, 1863 (1982).
23- M.B.Robin, Higher Excited States Of Polyatomic Molecules. Academic Press, New-york, 1974.
24- M.Bolle, K.Luther, J.Troc., Appl.Surface.Science 46 (1990) pp 279-283.
25- J.H.Branon, J.R.Lankard, A.I.Baise, Burns, and J.Kaufman, J.All.Phys,58(2), (1985) pp 20-36.
26- J.E.Andrew, P.E.Dyer, D.Forster, and P.H.Key, Appl. Phys. Lett, 43(8), (1983) pp 717-
27- T.F.Deutsh, and M.W.Geis, J.Appl.Phys 54(12), (1983) pp 7201-
28- H.Hg. Jellinek, R.Srinivasan, J.Phys.Chem 88(4), (1984) pp 3048-
29- R.Srinivasan, B.Braren, J.Polym. Ed.22, 2601 (1984).
30- R.Srinivasan, B.Braren, D.Seeger, R.W.Dreyfus (to be Published).
31- R.Srinivasan, R.W.Dreyfus, Proceeding of the Seventh International Conference on Laser Spectroscopy (Springer-Veriag) (1985).
32- R.Cestler, N.S.Nogar, Appl.Phys.lett 49(18) (1986) pp 1175-
33- T.Yeh- Private Communication-
34- T.Yeh, J.Vac.Sci.Tecnol A4(3)- May-june (1986) pp 653-
35- G.Koren, T.Yeh, Appl.Phys.lett(44), (1984) pp 1112-
36- G.Koren, T.Yeh, J.Appl.Phys, 56 (1984), pp 2120-
37- G.M.Davis, M.C.Gower, C.Fatakis, T.Eftiniopoulos, A.Argyrakis, Appl. Phys A(36), 27 (1985).
38- R.Srinivasan, S.Lin -Private Communication-
39- B.Danielzik, N.Fabricius, M.Rowenkamp, D.Vonderlide, Appl.Phys.Lett 48(3), (1986).
40- S.G.Hansen, J.Appl.Phys 66(3), (1989).
41- G.Ulmer, B.Hasselberger, H.G.Busman, EEB Campbell, Appl.Surf.Science 46(1990),pp 272-278.
42- S.G.Hansen, J.Appl.Phys 66(3) (1989).
43- Dyer, J.Sidhu, J.Appl.Phys. 57 (1985) pp 1420-
44- Gotodetsky, T.G.Kazyaka, R.J.Melcher, R.Srinivasan, Appl.Phys.Lett (46), (1985), pp 828-
45- R.Srinivasan, B.Baren, D.Seeger and R.W.Dreyfus (to be published).
46- Journal. Of. America. Soc, Vol 106, no 105 (1984), pp 4289-
47- S.Deshmukh, E.W.Rothe, J.Appl.Phys 66(3), (1989) pp 1370-
48- J.O.Choi, J.A.Moore, J.C.Corelli, J.P.Silverman, H.B., Journal of Vaccumm and Technology (B), 6(3), (1988). pp 2286-2289
49- A.Heuberger, J.Vaccum and Technolgy (B), 6(1), (1988) pp 107-
50- M.Rotschild and all, J.Vac.Tec (B), 6(1), (1988) pp- 1
51- S.V.Babu, G.C.D'Coulo, F.D.Egitto, J.Appl.Phys, Vol 72, no 2, 15 July (1992), pp 692-698.

Polymer	a(cm^{-1})	Penetration Depth(μm)
PVF_2	$5.7*10^2$	80
PMMA	$2.0*10^3$	--
PVC	$7.6*10^3$	6.0
PET	$2.0*10^4$	--
PI	$1.0*10^5$	--
PS	$8.0*10^5$	0.058

TABLE.1. ABSORTION COEFFICIENT AND PENETRATION DEPTH OF UV(99%ENERGY)

λ(nm) / 10^4(cm^{-1})	193	248	308
PI	13(d)-45(c)	14(d)-45(b)	8(d)-26(b)
PET	12(d)	10(d)	2(d)
PVC	≅0.8	≅0.05	≅0.05
PMMA	0.5(f)	0.1(f)	--
PS		≅3	0.05
PVF_2	$3*10^2$	≅0.05	≅0.1
PE	$7*10^2$	≅0.05	≅0.05
PP	$5.5*10^2$	≅0.05	≅0.05

TABLE.2. Absorption Coefficient at Different Wavelength.

[b]-from 36,[c]-from39, [d]-from 43, [e]-from 44, [f]-from fig.20

λ(nm) / Φ(mj/cm2)	193	248	308
PI	0.03(a) 0.025(b)	0.01(a) 0.055(b)	0.115(b) 0.042(a)
PET	0.028(a)	0.03(a)	0.17(a)
PMMA	0.01(c)	0.01(c)	--
PC	0.06	--	--

Table.3. Values Of The Threshold Fluence For Different Polymers The duration of The Pulse is ≅ 30 ns

[a]-from 43, [b]-from 44 , [c]-from 45 .

Polymer	Index Of Refraction
PMMA	1.49(a)
PC	1.585(a)
PET	1.576(a)
PI	1.695(b)

Table.4. Index Of Refraction Of Different Polymers.

[a]-From 42 , [b]-From 35

Carbon Atom	Core Level Position[a]	Experimental Data[b]
C(Ph-H)	0.00	0.00
C(Ar-C=O)	+0.98	--
C(Ar-H)	+1.09	+1.13
C(Ph-N)	+1.25	--
C(C=O)	+4.05	+3.96

Table.5. a) All Values Are Relative To 300.5 ev.

b) All Values Are Relative To 284.0 ev.

polymer	a	b	e
PT	1 (1.08)	2.00	0.70
PI	1 (0.70)	2.10	0.57
PMMA	1 (1.10)	1.35	1.05

TABLE.7. Ratio Of The Oxygen To Carbon [O]/[C] XPS 1s Peak for PET, PI, PMMA For Various Treatment.[46]

a- simple as received.

b- exposed 10 mn at λ = 185 nm.

e- irradiated with three pulses (28 ns) from an ArF excimer laser (λ = 193 nm) with an intensity range of 150 mJ/cm2

· The number in parentheses are the measured ratios- all the values are normalized to 1 for the untreated surface.

Polymer	Mass	Possible Composition	Polymer	Mass	Possible Composition
PI	128	$C_{10}H_8^+C_9H_4O^+$	PET	78	$C_6H_6^+$
	78	$C_6H_6^+$		56	Fe^+
	126	$C_{10}H_6^+$		128	$C_{10}H_8^+C_9H_4O^+$
	50	$C_4H_2^+$		126	$C_{10}H_6^+$
	39	$C_3H_3^+$		154	$C_{12}H_{10}^+C_{11}H_6O^+$
	51	$C_4H_3^+$		104	$C_8H_8^+C_7H_4O^+$
	94	$C_6H_6O^+C_5H_4NO^+$		92	$C_7H_8^+C_6H_4O^+$
	63	$C_5H_3^+$		140	$C_{11}H_8^+C_{10}H_4O^+$
	74	$C_6H_2^+$		116	$C_9H_8^+C_8H_4O^+$
	140	$C_{11}H_8^+C_{10}H_4O^+$		118	$C_9H_{10}^+C_8H_6O^+$
	154	$C_{12}H_{10}^+C_{11}H_6O^+$		166	$C_{13}H_{10}^+C_{12}H_6O^+$
PC	128	$C_{10}H_8^+C_9H_4O^+$			
	126	$C_{10}H_6^+$			
	118	$C_9H_{10}^+C_8H_6O^+$			
	140	$C_{11}H_8^+C_{10}H_4O^+$			
	142	$C_{11}H_{10}^+C_{10}H_6O^+$			
	78	$C_6H_6^+$			
	154	$C_{12}H_{10}^+C_{11}H_6O^+$			
	116	$C_9H_8^+C_8H_4O^+$			
	94	$C_6H_6O^+$			
	104	$C_8H_8^+C_7H_4O^+$			
	92	$C_7H_8^+C_6H_4O^+$			
	120	$C_8H_8O^+$			
	166	$C_{13}H_{10}^+C_{12}H_6O^+$			
	108	$C_7H_8O^+C_6H_4O_2^+$			
	102	$C_8H_6^+C_7H_2O^+$			

Table.6. Majors Ions Observed With λ = 248 nm.

Figure Captions.

Fig.1.

a- UV Absorption Curves Of PE, PP, PVF_2.
b- UV Absorption Curves Of PVC and PS.

Fig.2.

a- PVC Ablation Threshold measured by QCM Method.
b- PS Ablation threshold measured by QCM Method.

Fig.3.

a- C_{1s} Spectrum Curve Fit Of Untreated PVF_2.
b- C_{1s} Spectrum of PVF_2 after Laser Treatment At Different Fluences:
   a- Untreated.
   b- 100 mJ/cm^2.
   c- 200 mJ/cm^2.
   d- 400 mJ/cm^2.

Fig.4.

a- Surface Atomic Ratio of $C-F_2$, $C-CF_2$ and C neutral for PVF_2 after laser treatment.
b- Surface Atomic Ratio Of [F]/[C] and [O]/[C] for PVF_2 after laser treatment.

Fig.5.

- C1S Spectrum of PVC before laser treatment.

Fig.6.

- Surface atomic ratio of Cl, O and C in PVC after laser treatment.

Fig.7.

- "Shake-Up" Structure and C-O links in C_{1s} spectrum of PS after laser treatment.
a- Untreated.
b- 20 mJ/cm_2.
c- 50 mJ/cm_2.
d- 70 mJ/cm_2.

FIG.8.

- C1S Spectra of PS after laser treatment.
a- Untreated.
b- 20 mJ/cm_2.
c- 50 mJ/cm_2.
d- 70 mJ/cm_2.
e- 100 mJ/cm_2.

Fig.9.

- Aromaticity, relative number of C-O links in C_{1s} and Surface atomic ratio of O and C in PS after laser treatment.

Fig.10.

-C_{1s} Spectra of PI before laser treatment.

Fig.11.

-C_{1s} Spectra of PI after laser treatment:
a- 6.0 mJ/cm².
b- 18 mJ/cm².
c- 28 mJ/cm².
d- 72 mJ/cm².

Fig.12.

- Variation of C_{1s} Phen/C_{tot}; CN and C=C/C_{tot}; C=C/C_{tot} ratios after laser treatment as a function of the fluence.

Fig.13.

-Variation of [N]/[C] atomic ratio versus laser fluence in PI.

Fig.14.

-XPS C_{1s} and O_{1s} of PET

Fig.15.

-XPS C_{1s} and O_{1s} of PET with curve-fitted components.

Fig.16

-XPS [O]/[C] atomic ratio of PET.

Fig.17.

-Variation of Absorption Coefficient with wavelength

for PMMA

Fig.18.

-Absorption Spectra of PI at different wavelength..

Fig.19.

-Fluence dependence of the ablation rate at various wavelengths for PMMA-1%DPT; at 193 and 248 nm.

Fig.20.

-Formulas of four polymers :(A) PMMA, (B) PI, (C) PC, (D) PET.

Fig.21.

-Etch depth vs number of pulses for PMMA and PC at an average fluence of 1.6 mJ/cm².

Fig.22.

-Etch depth of PI versus fluence for different laser pulse (, 193; , 248; ,308 nm).

Fig.23.

-Etch rate versus incident fluence in Air at (248 ,308, 351nm) for PI .

Fig.24.

-Energy-level diagram for hypothetic bond X-Y.

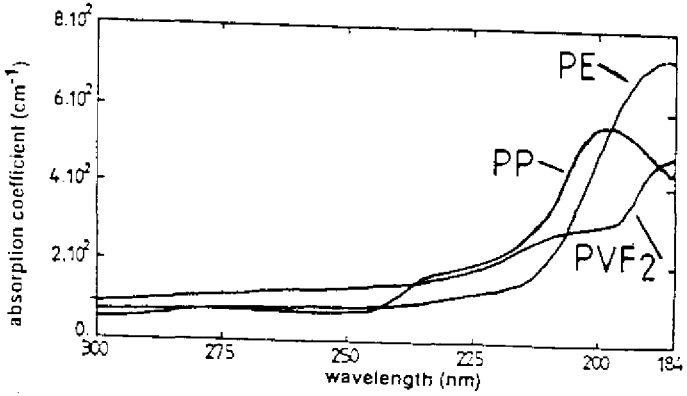
absorption coefficient (cm⁻¹)
8.10²
6.10²
4.10²
2.10²
0
PE
PP
PVF2
300
275
250
225
200
184
wavelength (nm)

FIG.Ia.

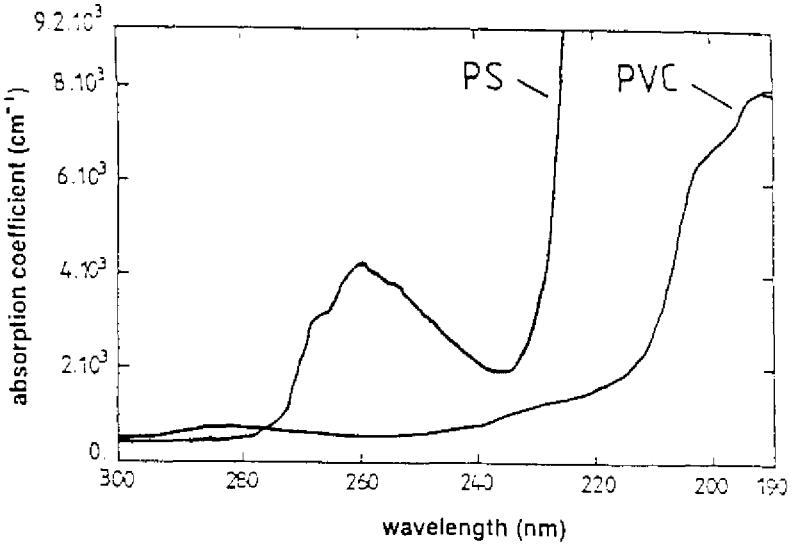
absorption coefficient (cm⁻¹)
9.2.10³
8.10³
6.10³
4.10³
2.10³
0
PS
PVC
300
280
260
240
220
200
190
wavelength (nm)

FIG.Ib.

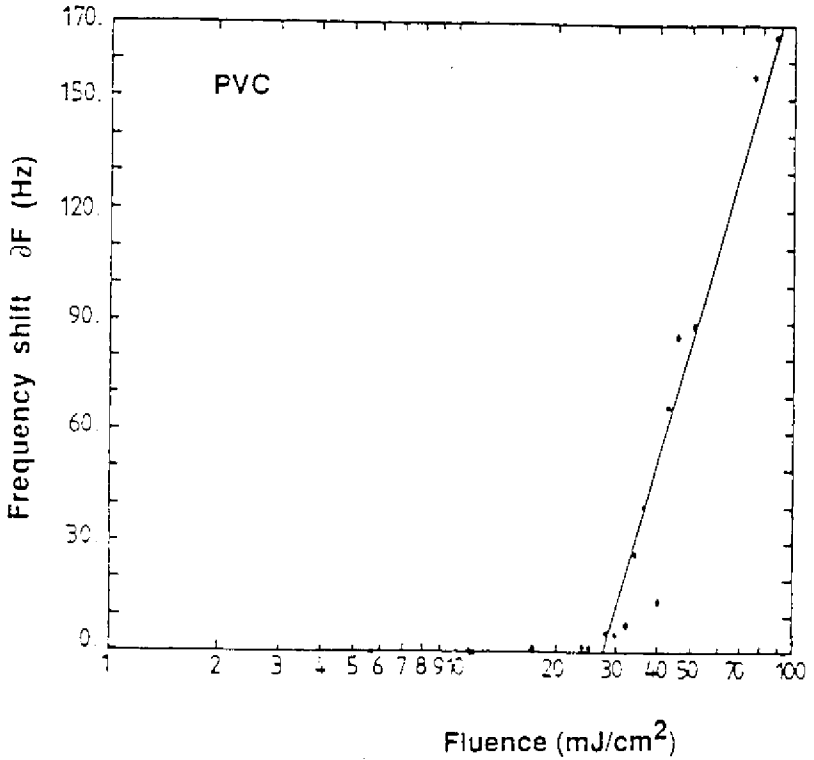
PVC
Frequency shift ∂F (Hz)
170.
150.
120.
90.
60.
30.
0
1
2
3
4
5
6
7
8
9
10
20
30
40
50
70
100
Fluence (mJ/cm2)

FIG.2a.

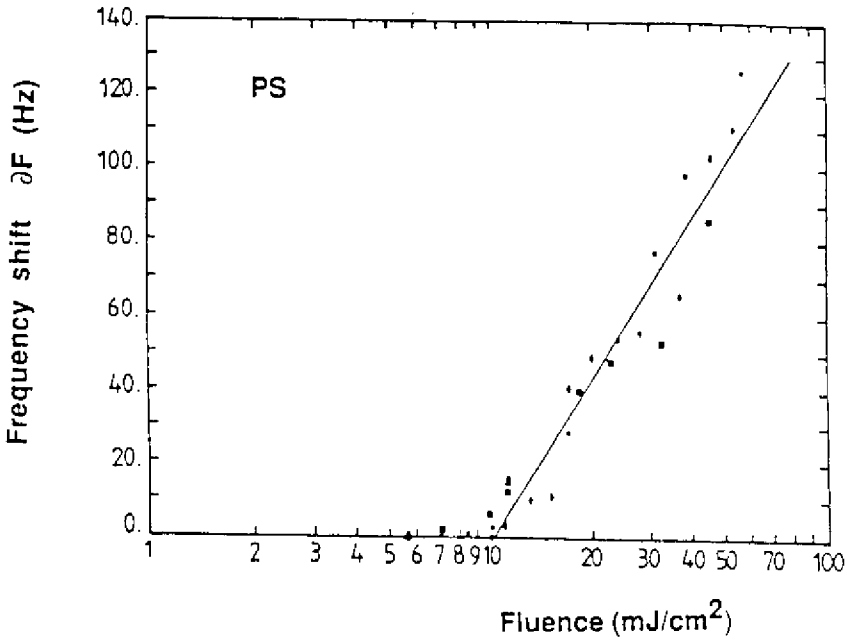
PS
Frequency shift ∂F (Hz)
140.
120.
100.
80.
60.
40.
20.
0.
1
2
3
4
5
6
7
8
9
10
20
30
40
50
70
100
Fluence (mJ/cm2)

FIG.2b.

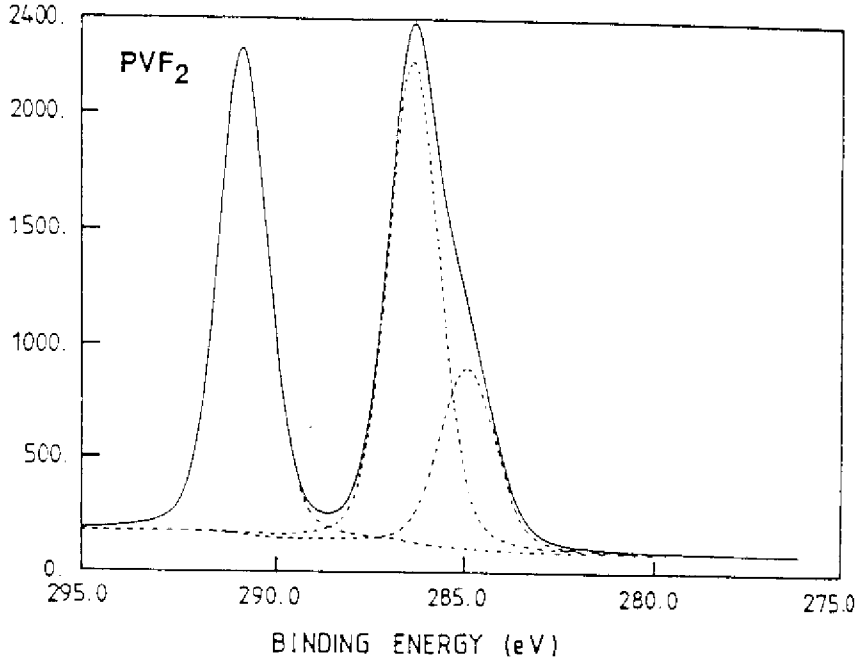
PVF2
2400.
2000.
1500.
1000.
500.
0
295.0
290.0
285.0
280.0
275.0
BINDING ENERGY (eV)

FIG.3a.

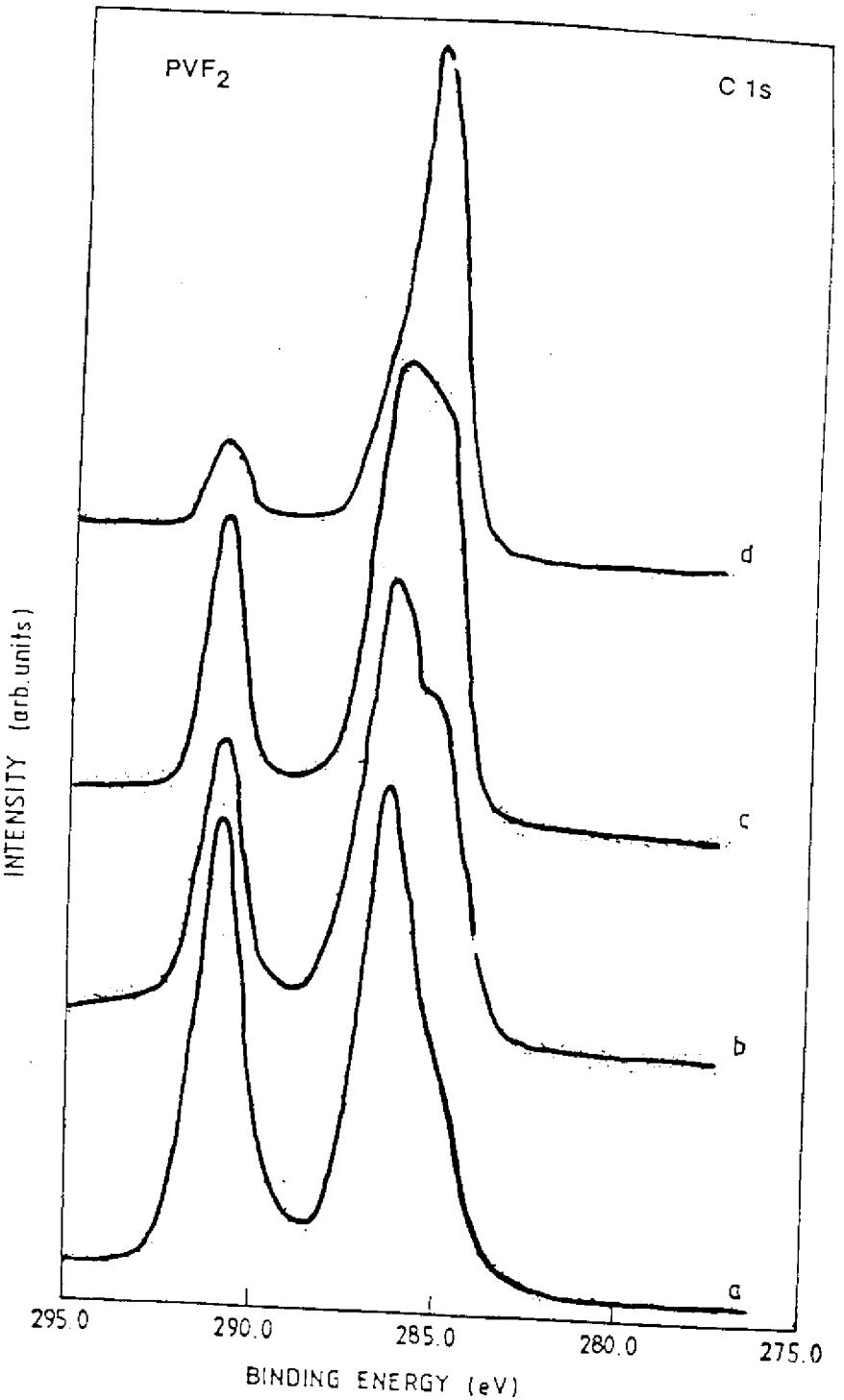
PVF2
C 1s
INTENSITY (arb.units)
d
c
b
a
295.0
290.0
285.0
280.0
275.0
BINDING ENERGY (eV)

FIG.3b.

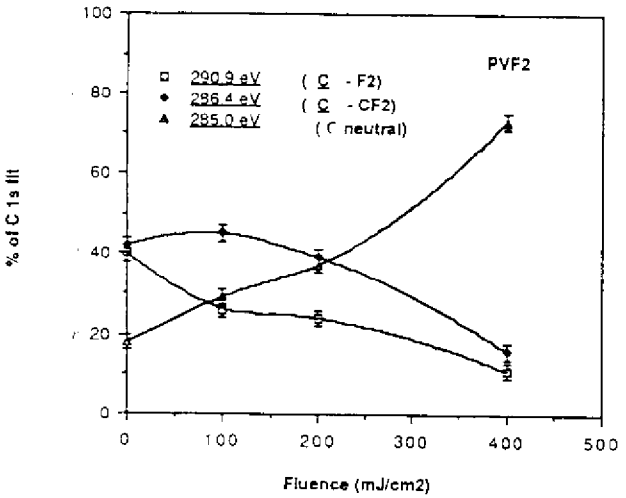
PVF2
290.9 eV (C - F2)
286.4 eV (C - CF2)
285.0 eV (C neutral)
% of C 1s fit
Fluence (mJ/cm2)
0
20
40
60
80
100
0
100
200
300
400
500

FIG.4a.

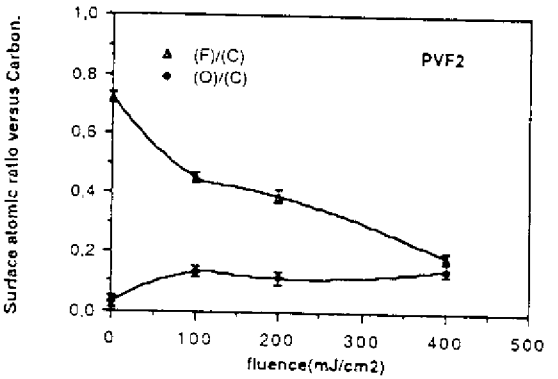
PVF2
(F)/(C)
(O)/(C)
Surface atomic ratio versus Carbon.
fluence(mJ/cm2)
0.0
0.2
0.4
0.6
0.8
1.0
0
100
200
300
400
500

FIG.4b.

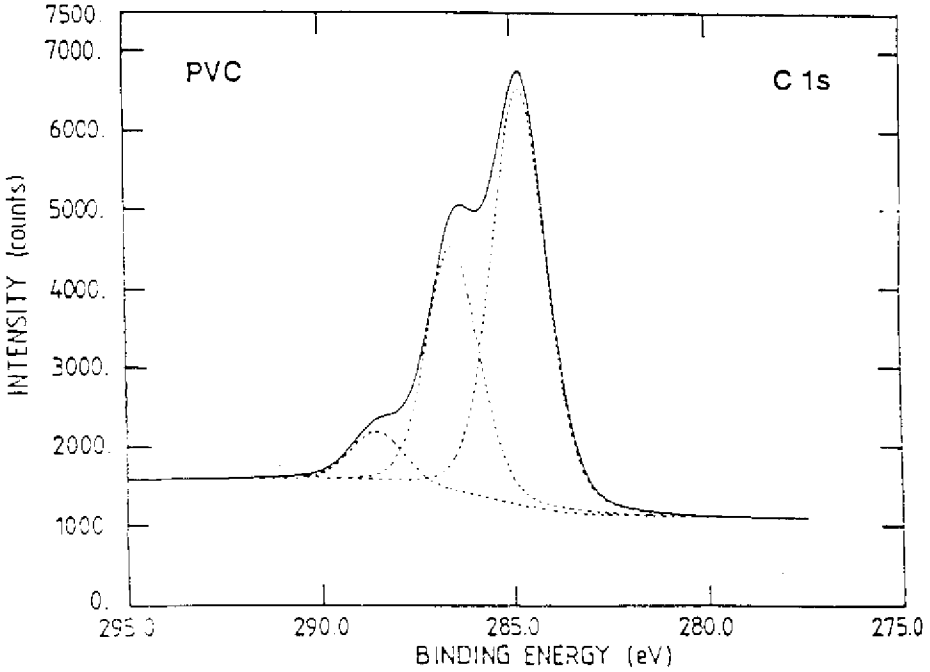
PVC
C 1s
INTENSITY (counts)
7500.
7000.
6000.
5000.
4000.
3000.
2000.
1000
0.
295.0
290.0
285.0
280.0
275.0
BINDING ENERGY (eV)

FIG.5.

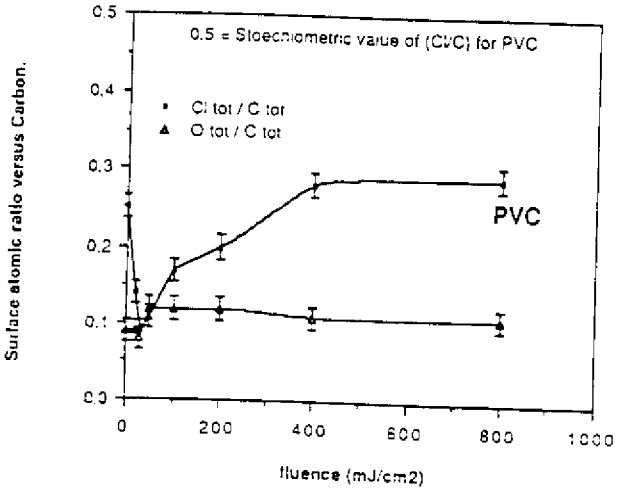
0.5 = Stoechiometric value of (Cl/C) for PVC
Cl tot / C tot
O tot / C tot
PVC
Surface atomic ratio versus Carbon.
0.5
0.4
0.3
0.2
0.1
0.0
0
200
400
600
800
1000
fluence (mJ/cm2)

FIG.6.

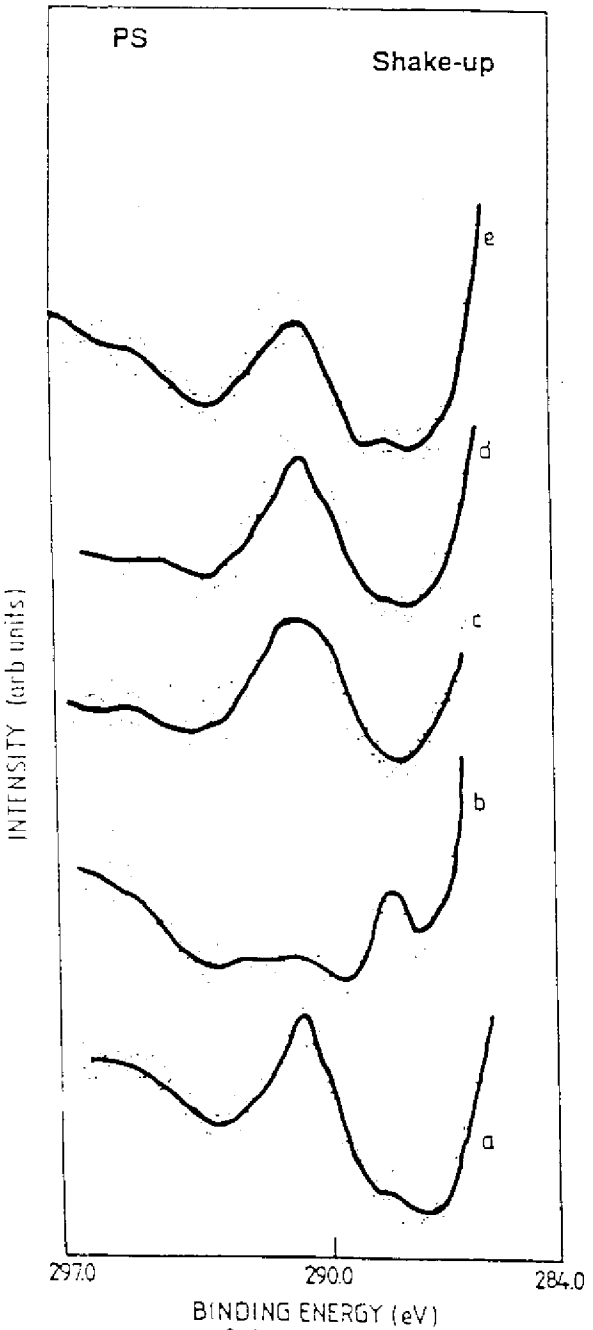
PS
Shake-up
e
d
c
b
a
INTENSITY (arb units)
297.0
290.0
284.0
BINDING ENERGY (eV)

FIG.7.

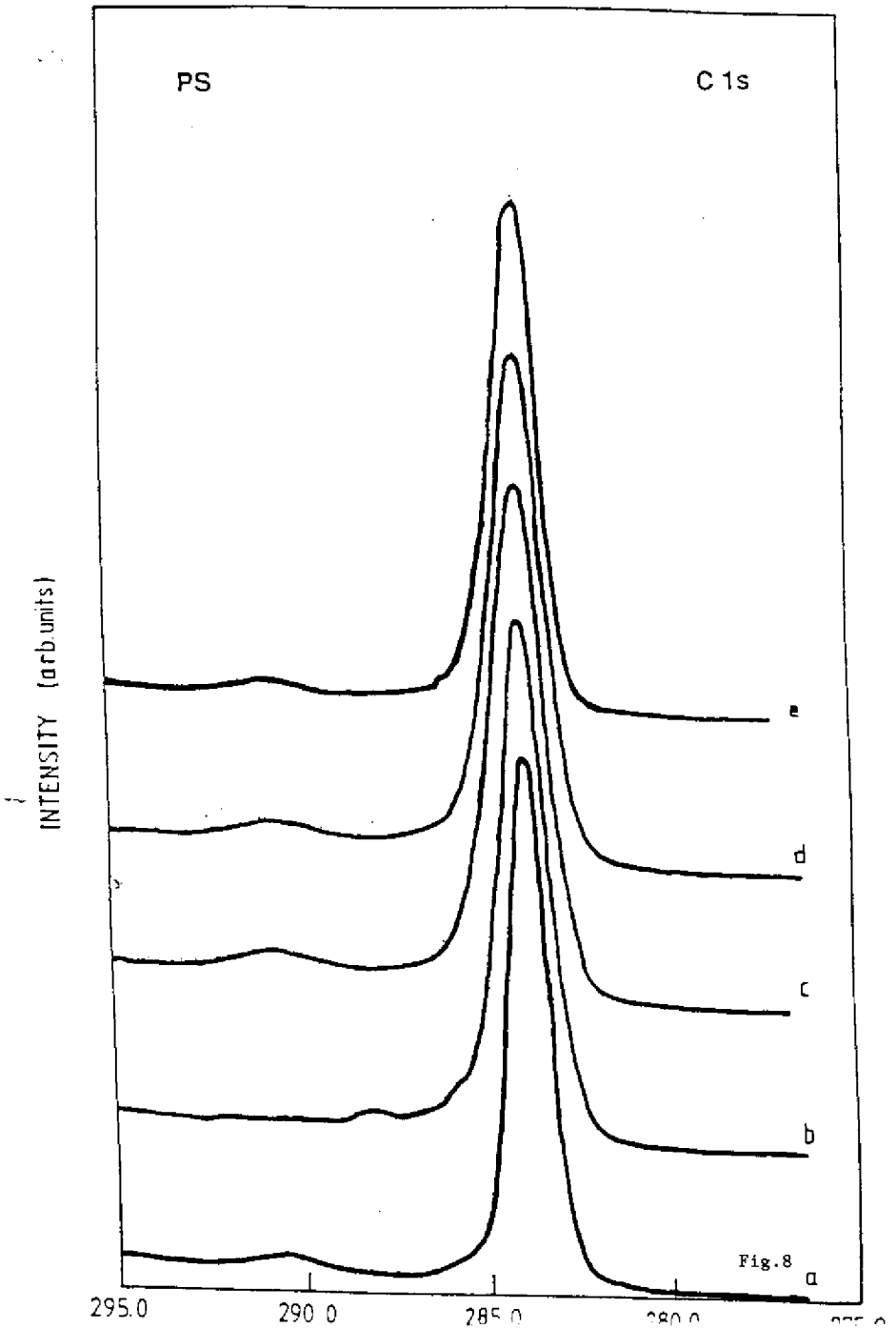
PS
C 1s
INTENSITY (arb.units)
e
d
c
b
a
295.0
290 0
285 0

Fig.8

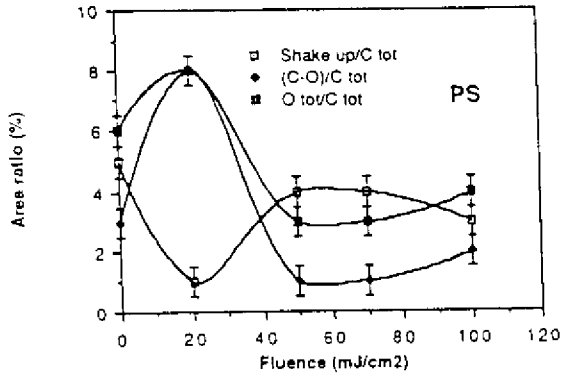

FIG.9.

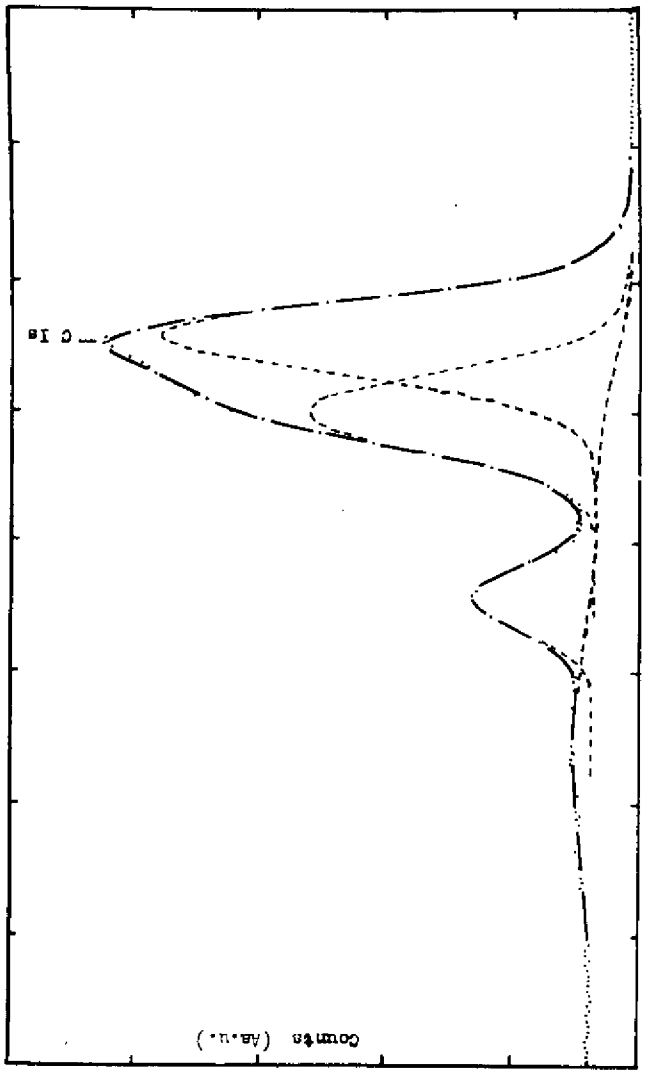

C_{1s}

FIG.10.

C_{1s}

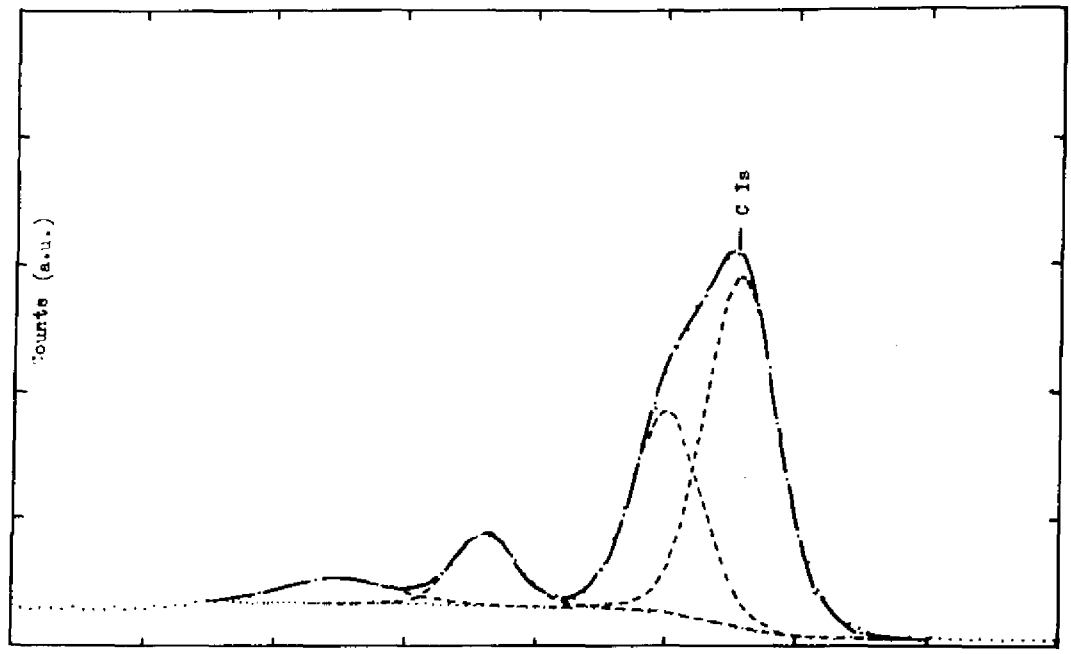

FIG.IIa.

C_{1s}

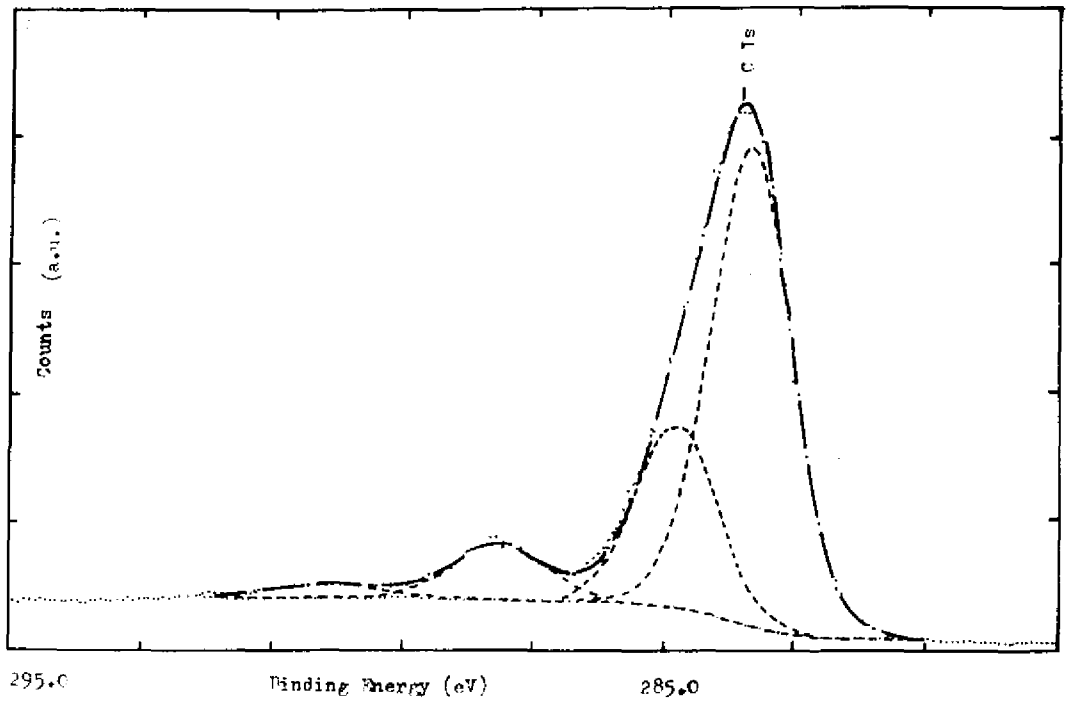

FIG.IIb.

C_{1s}

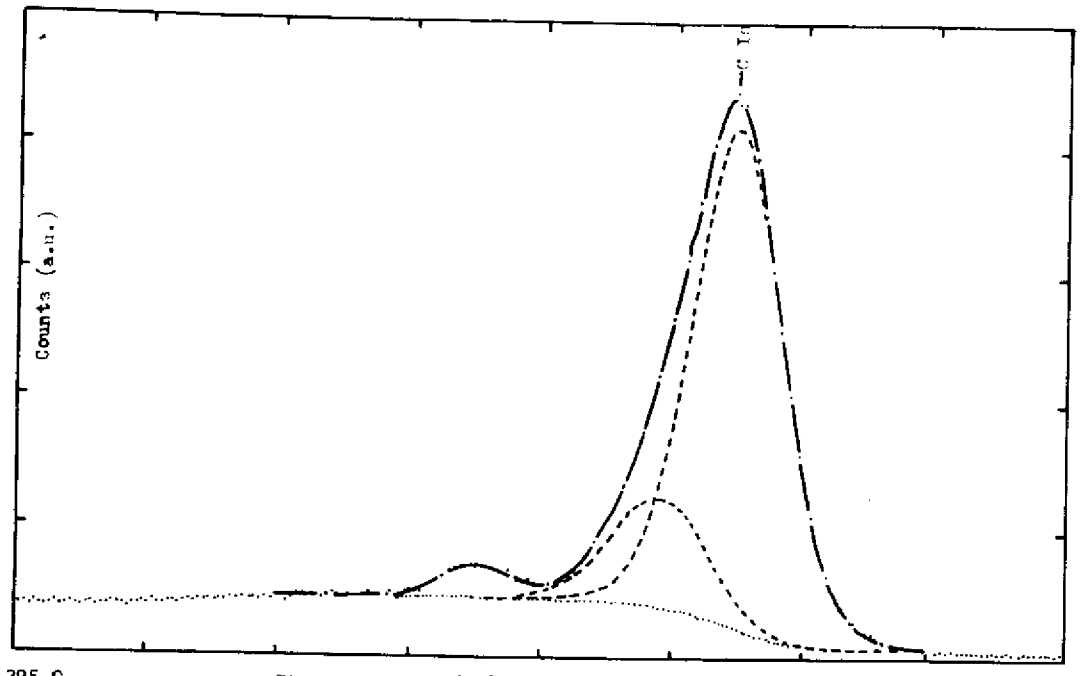

FIG.IIc.

C_{1s}

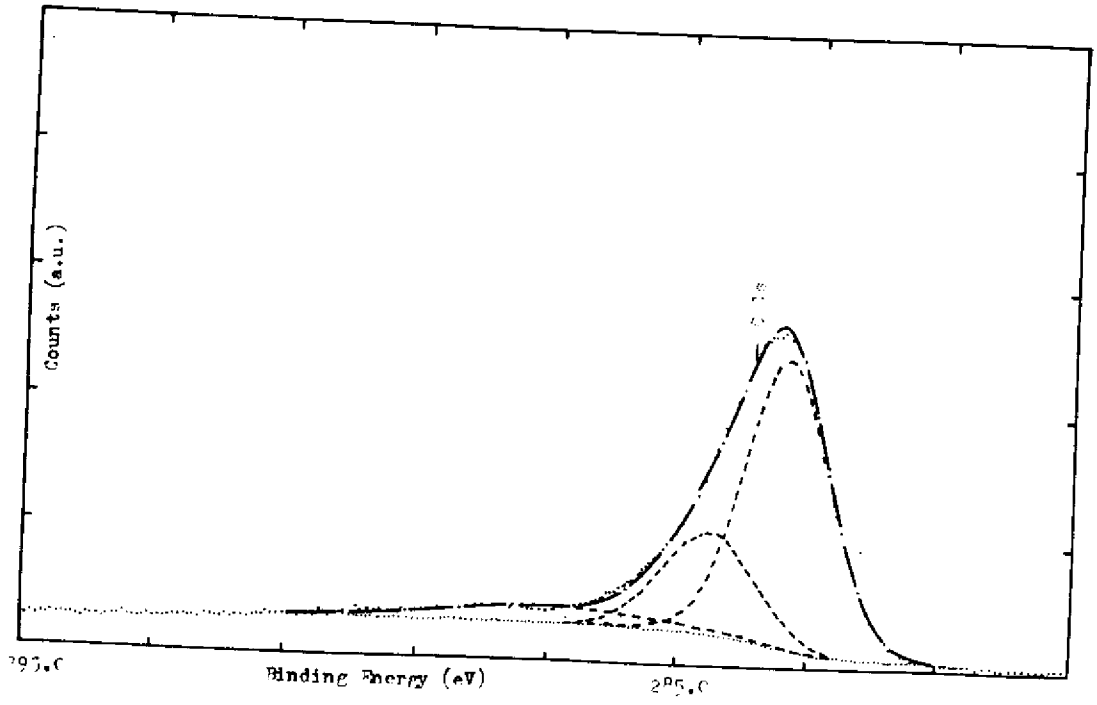

FIG.IId.

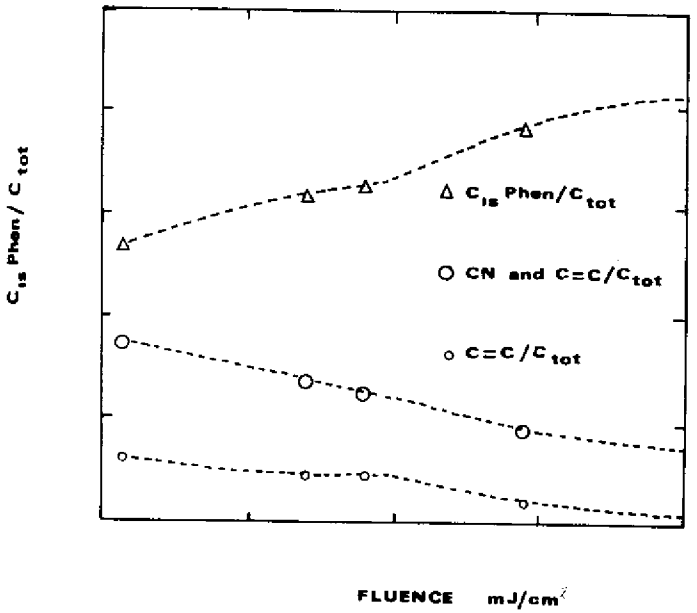
$C_{is\ Phen}/C_{tot}$
Δ $C_{is\ Phen}/C_{tot}$
O CN and C=C/C_{tot}
o C=C/C_{tot}
FLUENCE mJ/cm²

FIG.12.

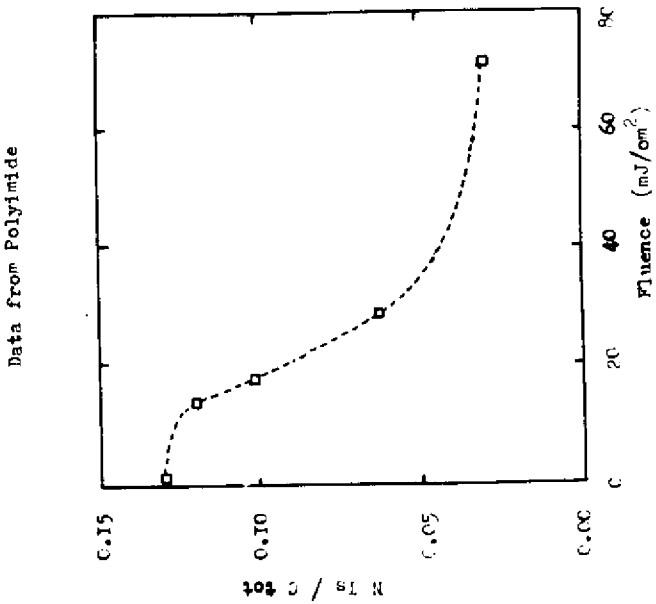
Data from Polyimide
N 1s / C tot
0.15
0.10
0.05
0.00
0
20
40
60
80
Fluence (mJ/cm²)

FIG.13.

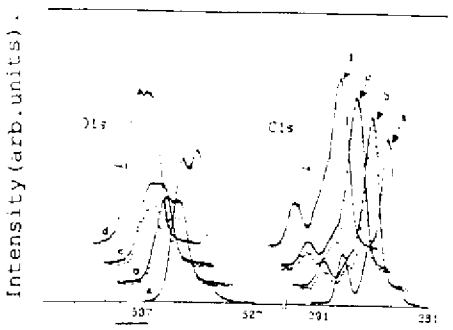

Fig.14 XPS C1s and O1s core level emission of PET surface: (a) PET as received. (b) PET irradiated with 1 laser pulse at 193 nm (100mj/cm2),. (c) PET irradiated with 1 laser pulse at 193 nm (450 mj/cm2)

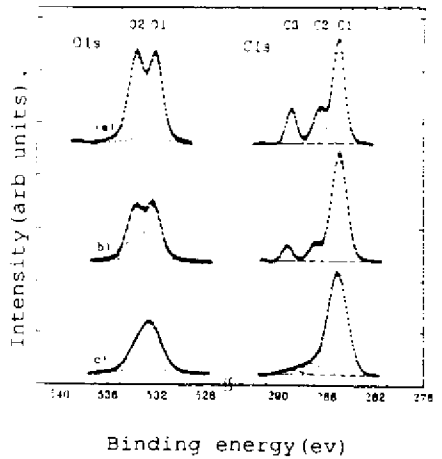

Fig.15. XPS C1s and O1s core level emissions of PET surface with curve-fitted components. (a) PET as received, (b) PET irradiated with one laser pulse at 193 nm (100mj/cm2), (c) PET irradiated with λ=185 nm (5h).

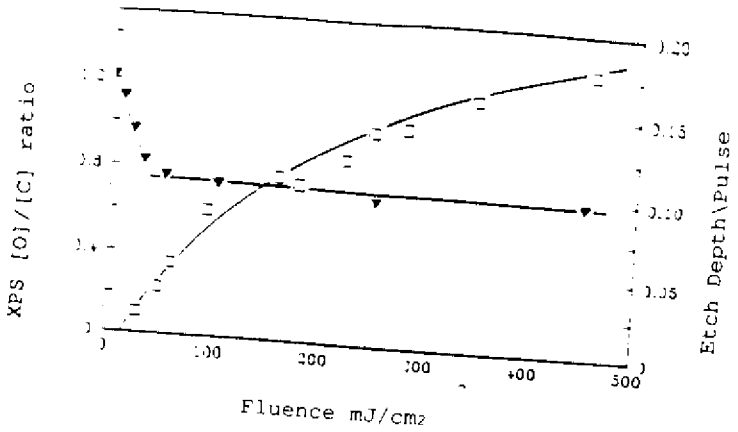

Fig.16. XPS O(1s)/ C(1s) emission ratio of irradiated PET (193nm) as a function of the pulse energy. (▼) XPS measurement after 1 pulse. (□) Etch depth per pulse as a function of the pulse energy.

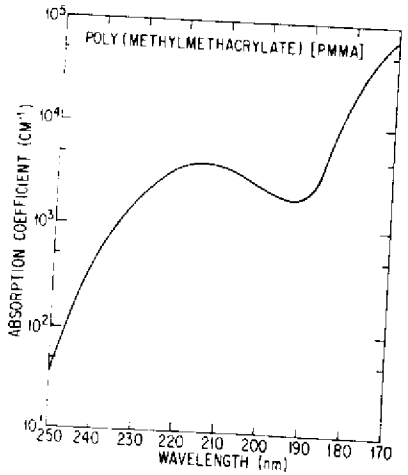

Fig.17. Variation of Absorption Coefficient With Wavelength.

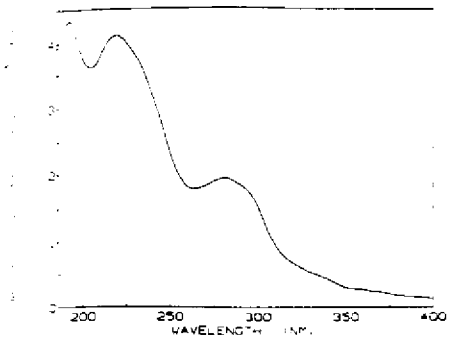

Fig.18.
-Absorption Coefficient of PI at Different Wavelength.

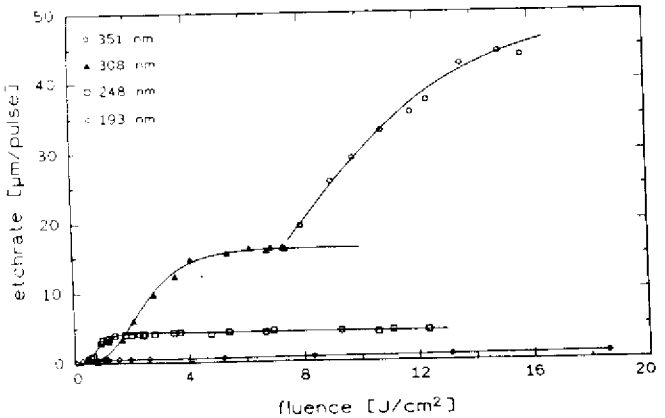

Fig.19. Fluence dependence of the ablation rate at various wavelength for PMMA-1%DPT; at 193 and 248 nm.

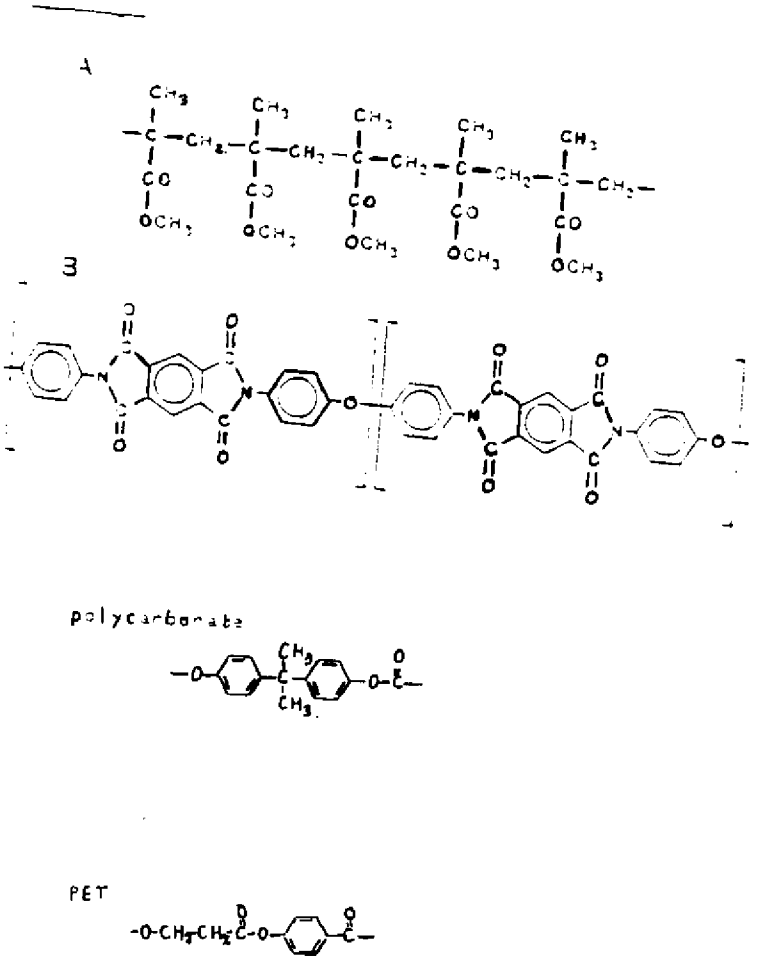

Fig.20. Formulas Of Four Polymers : (A) PMMA, (B) PI, (C) PC, (D) PET.

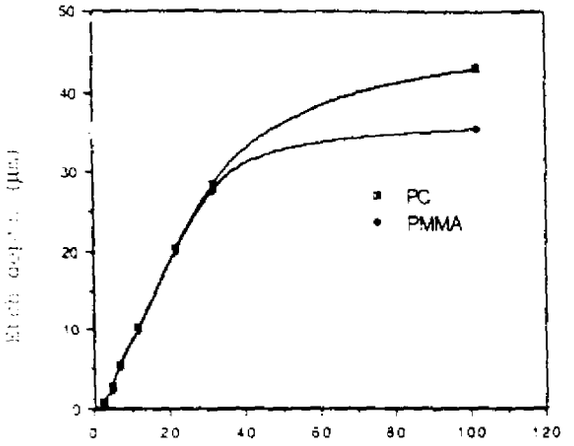

Fig.21. Etch Depth versus number of pulses for PMMA and PC.

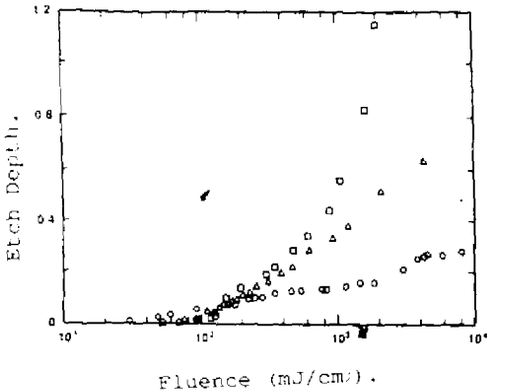

Fig.22. Etch depth/ pulse vs fluence for PI at (O ,193nm; Δ 248; □ 308nm).

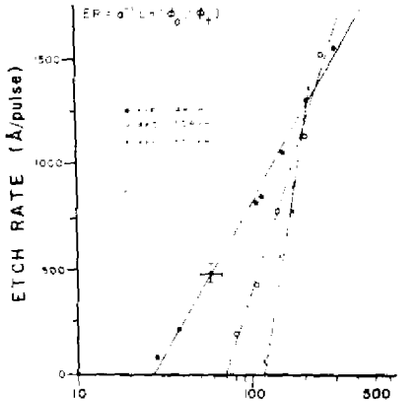

Fig.23. Etch rate versus Incident fluence for PI in Air.

plots of Experimentally measured single-pulse etch depth versus O... Etching in Air. The straight line are the 'best fit' of EQ.2. from [25].

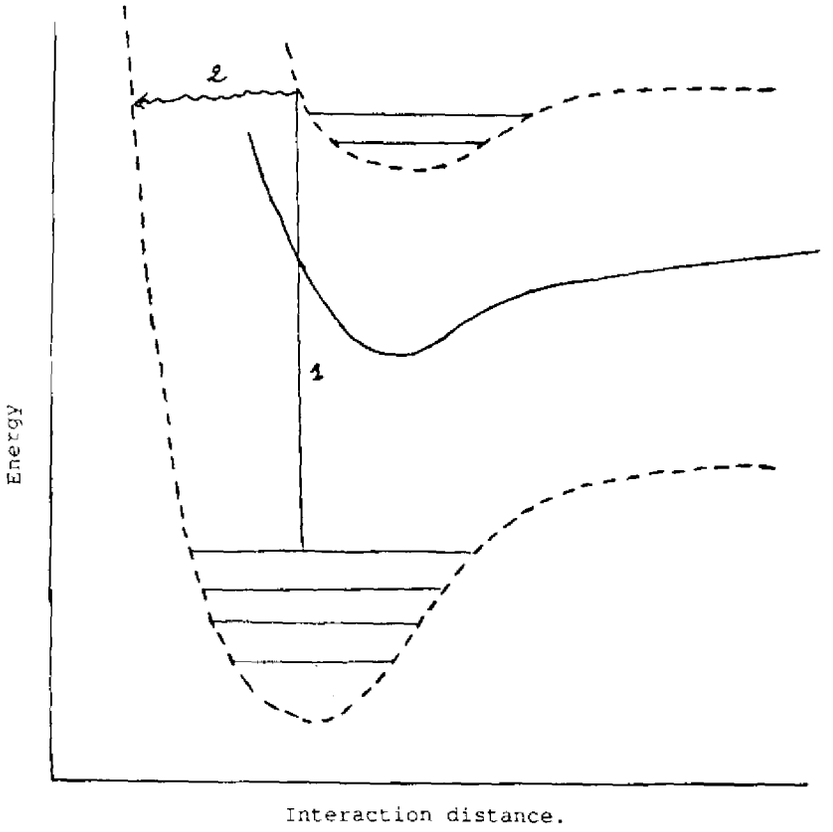

Fig.24. Energy-level diagram for hypothetical bond X-Y.
The lower broken line represents the ground electronic state, the upperbroken line and the solid line describe excited electronic states.